# Electronic Supplementary Information (ESI)

## A highly selective coumarin-based chemosensor for dual sensing of $Cu^{2+}$ and $Zn^{2+}$ ions with logic gate integration and live cell imaging

**Avanish Kumar Singh[a], Amit Kumar Singh[a], Sashikant Sharma[b], Vijay Kumar Sonkar[b] and V. P. Singh*[a]**

[a] Department of Chemistry, Institute of Science, Banaras Hindu University, Varanasi-221005 (India)

[b] Department of Molecular and Human Genetics, Institute of Science, Banaras Hindu University, Varanasi-221005 (India)

## Table of Contents

## Methods and measurements

### Limit of detection (LOD)

The limit of detection for **CIH** was determined using fluorescence titration data and the IUPAC definition based on a plot of emission intensity vs. increasing $Zn^{2+}/Cu^{2+}$ concentration. We repeated our observations eight times, measuring the emission intensity of **CIH** without $Zn^{2+}/Cu^{2+}$ at every repetition and calculated the standard deviation of blank data. Fluorescence intensity data at 509 nm against $Zn^{2+}/Cu^{2+}$ concentration were plotted to determine the slope. The detection limit is established using the following equation:[1]

$$\text{Limit of detection (LOD)} = \frac{3SD}{Slope(m)}$$

Where, the variables m, stands for the slope of intensity vs. sample concentration, and SD, stands for the standard deviation of blank readings.

### Binding constant (Ka)

Using the Job's plot, the binding ratio of **CIH** to metal ions was calculated. The Benesi-Hildebrand equation was used to determine the binding constants ($K_a$) of **CIH** for $Zn^{2+}$ and $Cu^{2+}$.[2]

$$\frac{I_o}{I - I_o} = \frac{a}{b - a}\left(\frac{1}{K_a[Metal]} + 1\right)$$

Where, I and $I_0$ represent the intensity of **CIH** fluorescence at 509 nm in the presence and absence of $Zn^{2+}/Cu^{2+}$, respectively; a and b are constants; and [Metal] represents the concentration of $Zn^{2+}/Cu^{2+}$.

### Fluorescence quantum yield measurements

The following equation was used to calculate quantum yield:[3]

$$Q = Q_r\left(\frac{I}{I_r}\right)\left(\frac{OD}{OD_r}\right)\left(\frac{n^2}{n_r^2}\right)$$

Where Q is the fluorescence quantum yield, I is the integrated fluorescence intensity, n is the refractive index of liquid, and OD is the optical density (absorption). The subscript r is used to represent the known quantum yield of reference quinine sulfate, which is 0.54 in 0.1 M $H_2SO_4$.

### Fluorescence decay measurements

To explore sensing properties, time-resolved fluorescence spectra were taken. The following equation has been used to calculate dynamic parameters:

$$y = A_1 * exp\left(-\frac{x}{\tau_1}\right) + A_2 * exp\left(-\frac{x}{\tau_2}\right) + y_0$$

The following equation was used for calculating the weighted mean lifetime:

$$<\tau>= (A_1\tau_1 + A_2\tau_2)/(A_1 + A_2)$$

Where, $\tau_1/\tau_2$ and $A_1/A_2$ are lifetimes ($\tau$) and the fractions or amplitudes (A), respectively.

The following equations are used to compute the radiative rate constant ($K_r$) and non-radiative rate constant ($K_{nr}$):[4]

$$<\tau^{-1} \geq \left(K_r + K_{nr}\right)$$

$$K_r = \frac{\Phi}{<\tau>}$$

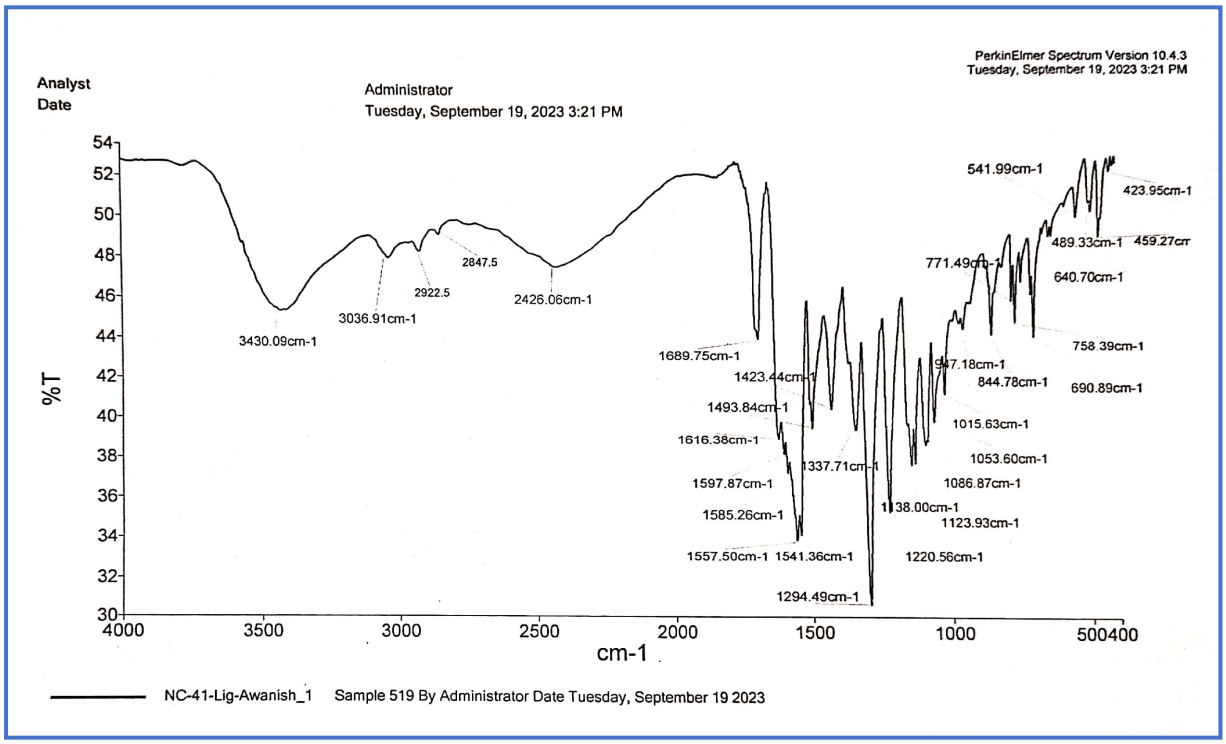

**Fig. S1** IR spectrum of **CIH**.

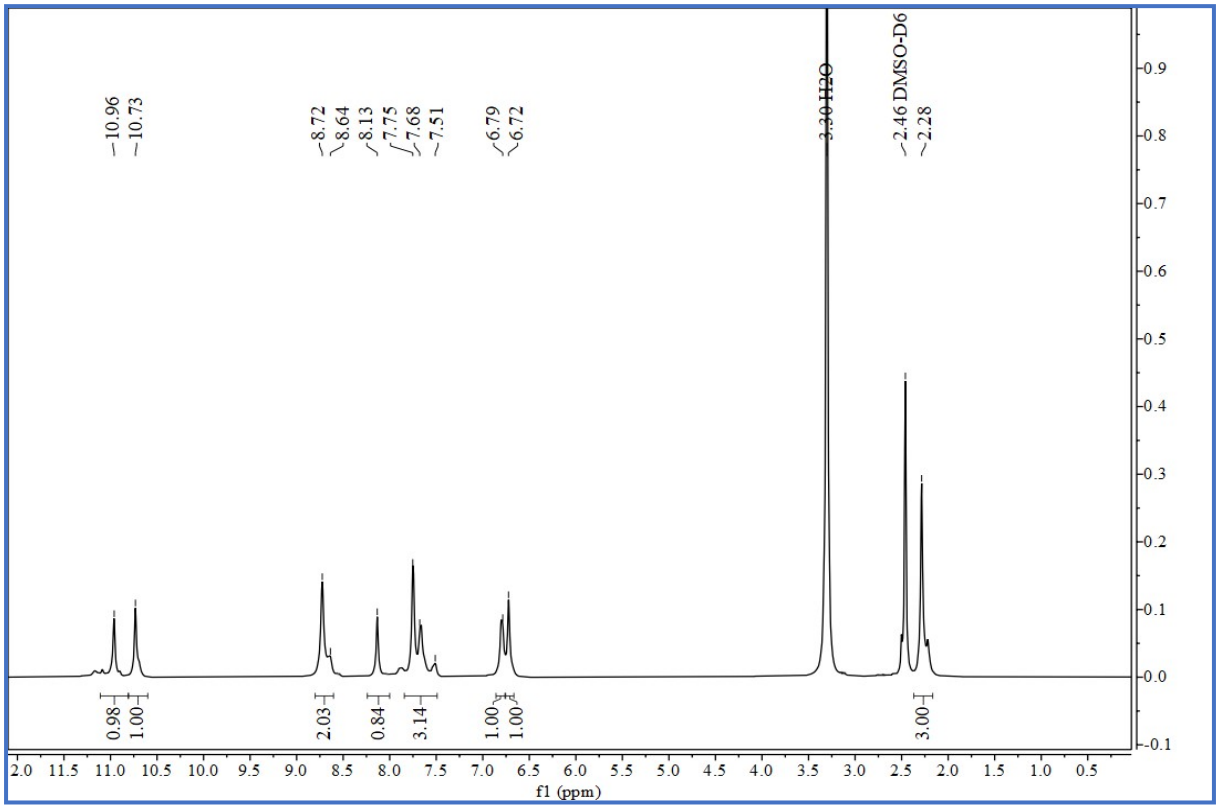


**Fig. S2** $^{1}$H NMR spectrum of **CIH**

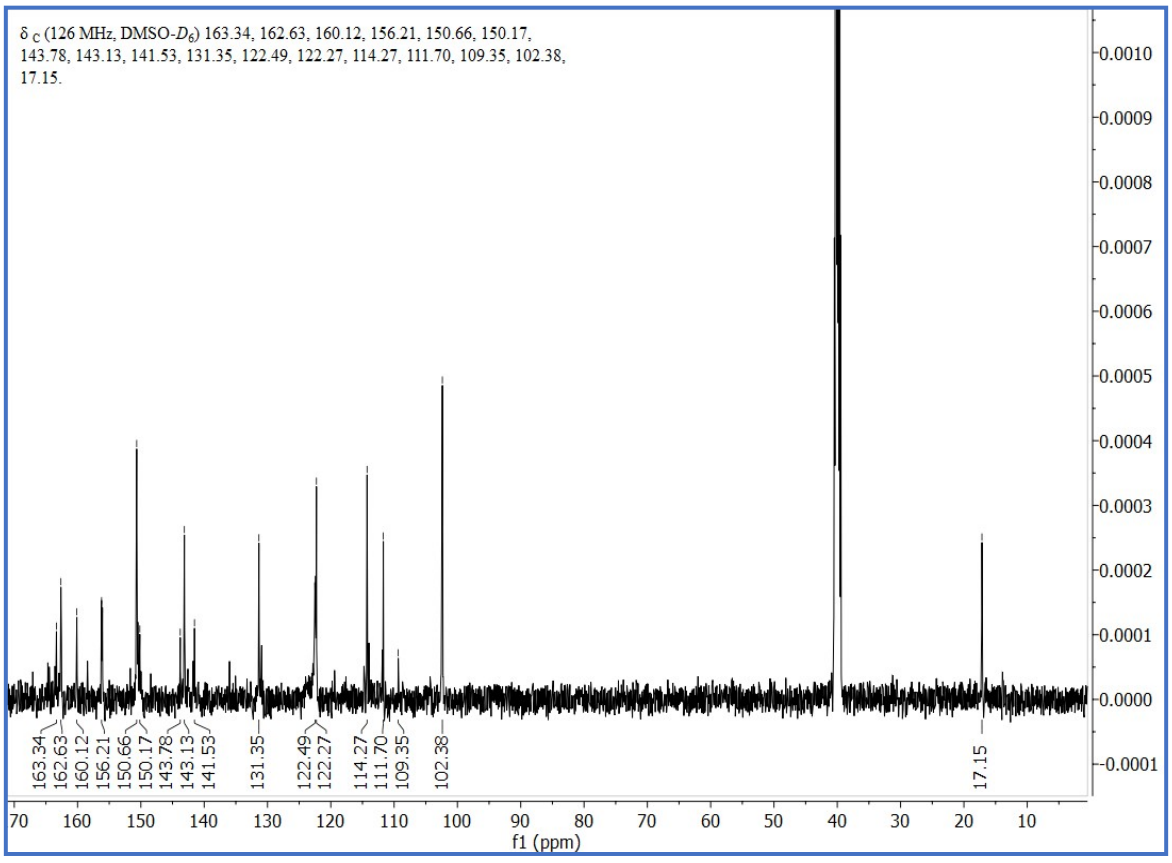

**Fig. S3** $^{13}C$ NMR spectrum of **CIH**

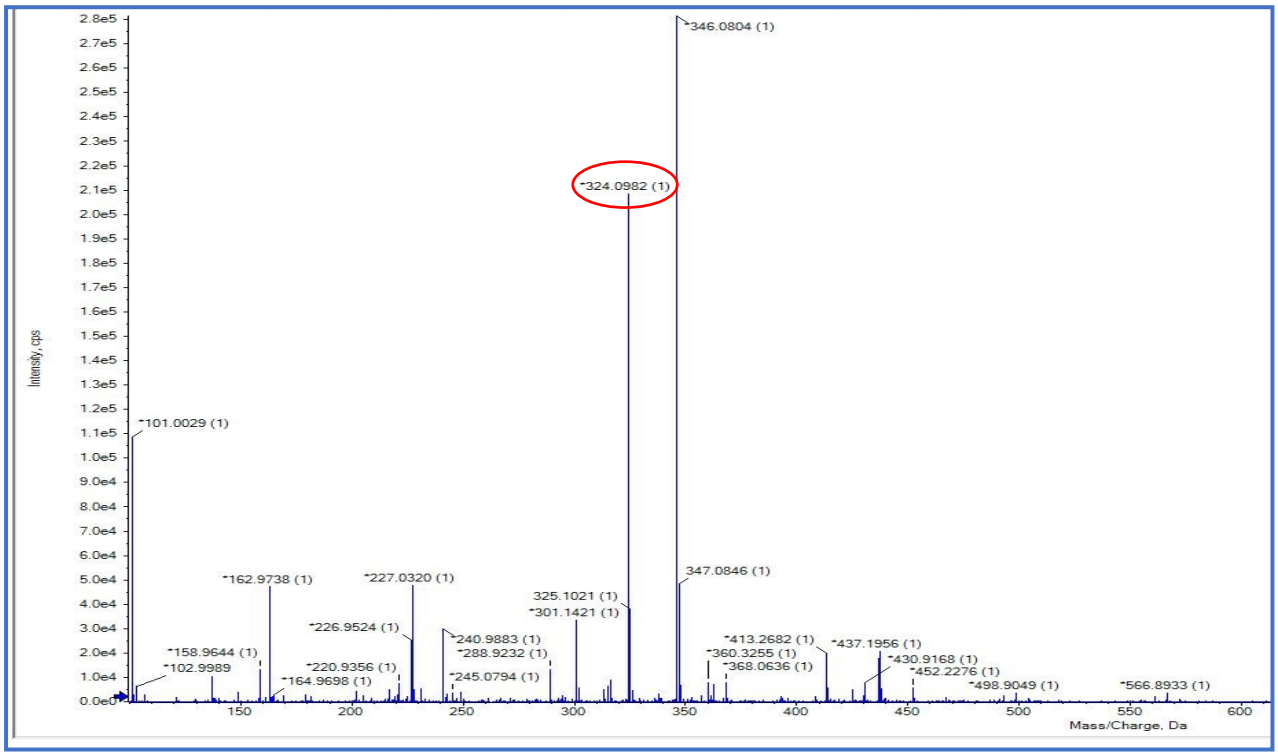


**Fig. S4** Mass spectrum of **CIH**

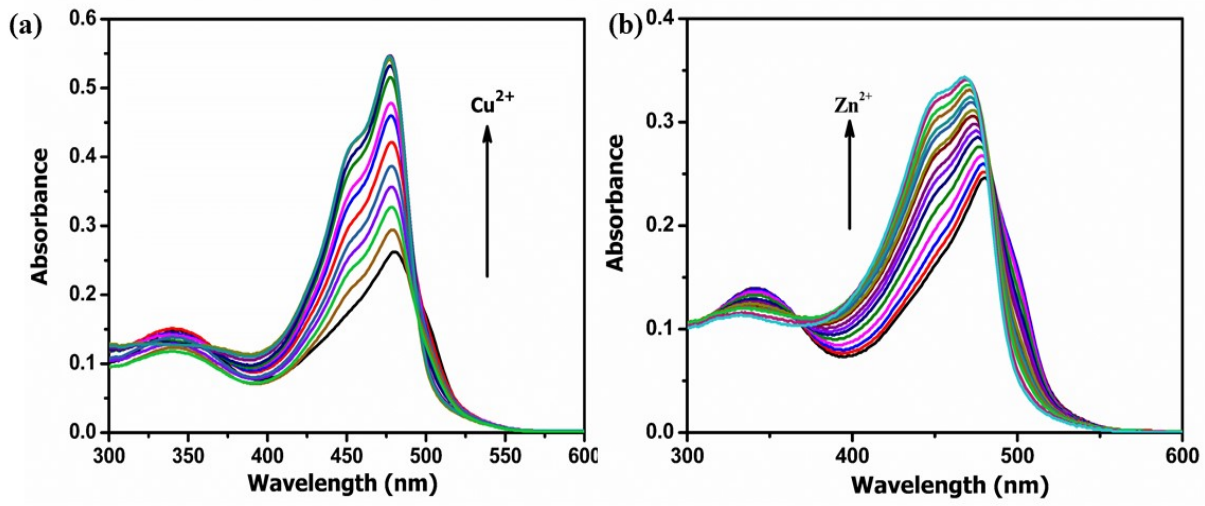


**Fig. S5** UV-Vis titration spectra of **CIH** (20 μM) in DMF:$H_2O$ (7:3, v/v, pH 7.4) HEPES buffer solution **(a)** in the presence of increasing concentration of $Cu^{2+}$ (0-1equiv.); **(b)** in the presence of increasing concentration of $Zn^{2+}$ (0-1equiv.).

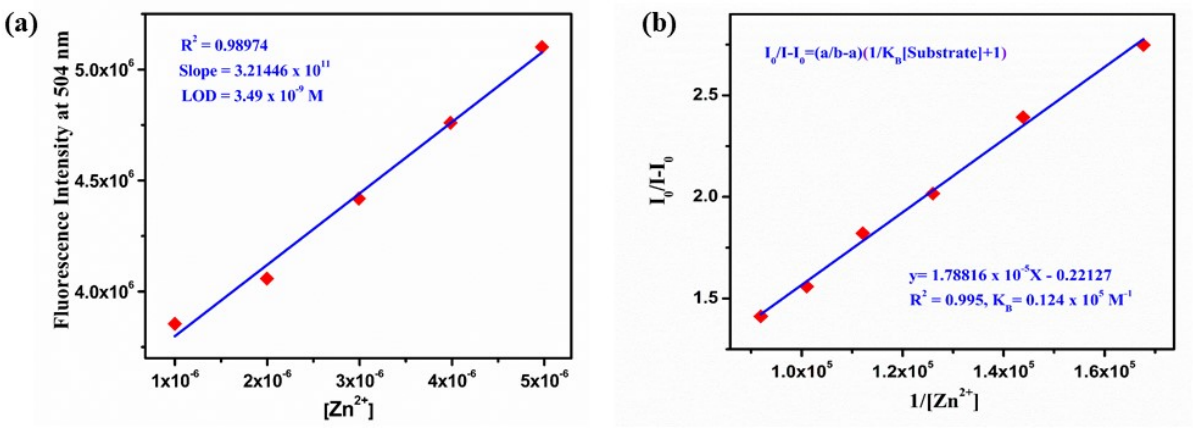


**Fig. S6 (a)** Limit of detection (LOD) plot, the change in fluorescence intensity at 504 nm of **CIH** (20 μM) as a function of $Zn^{2+}$ ions concentration **(b)** Benesi-Hildebrand plot of **CIH** for determination of binding constant with $Zn^{2+}$.

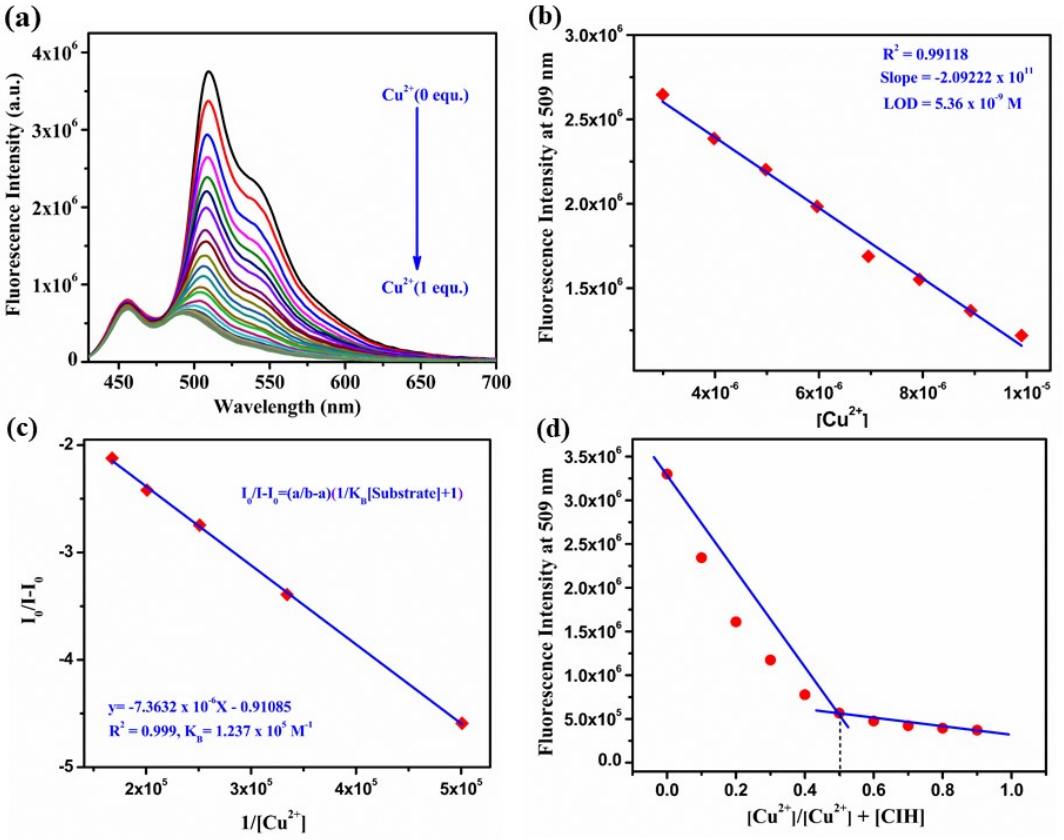


**Fig. S7 (a)** Fluorescence titration spectra of **CIH** (20 μM, λex = 420 nm) in DMF:$H_2O$ (7:3, v/v, pH 7.4) HEPES buffer solution in the presence of $Cu^{2+}$ (0- 1 equiv.) **(b)** Limit of detection (LOD) plot, the change in fluorescence intensity at 509 nm of **CIH** (20 μM) as a function of $Cu^{2+}$ ion concentration **(c)** Benesi-Hildebrand plot of **CIH** for evaluation of binding constant with $Cu^{2+}$ and **(d)** Job's plot for determination of binding stoichiometry for **CIH**-$Cu^{2+}$.

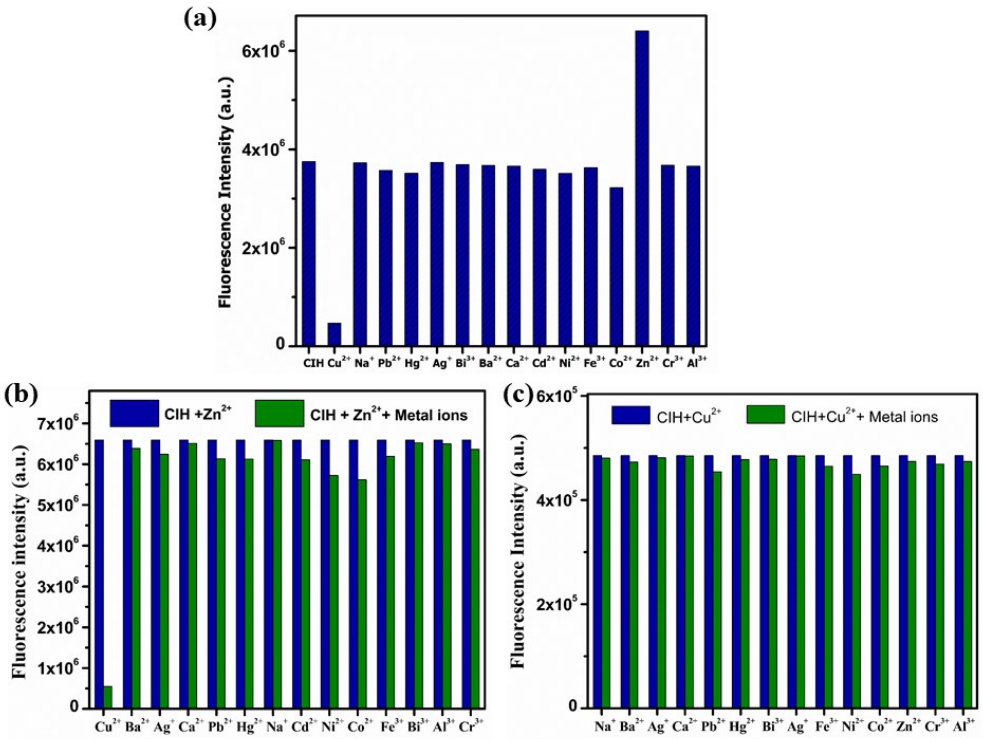


**Fig. S8** Fluorescence intensity measurement of **CIH** (20 μM) **(a)** after addition of various metal ions (20 μM) in DMF:$H_2O$ (7:3, v/v, pH 7.4) HEPES buffer solution **(b)** in the presence of $Cu^{2+}$ + other metal ions (20 μM) in DMF:$H_2O$ (7:3, v/v, pH 7.4) HEPES buffer solution **(c)** in the presence of $Zn^{2+}$ + other metal ions (20 μM) in DMF:$H_2O$ (7:3, v/v, pH 7.4) HEPES buffer solution. (λex = 420 nm).

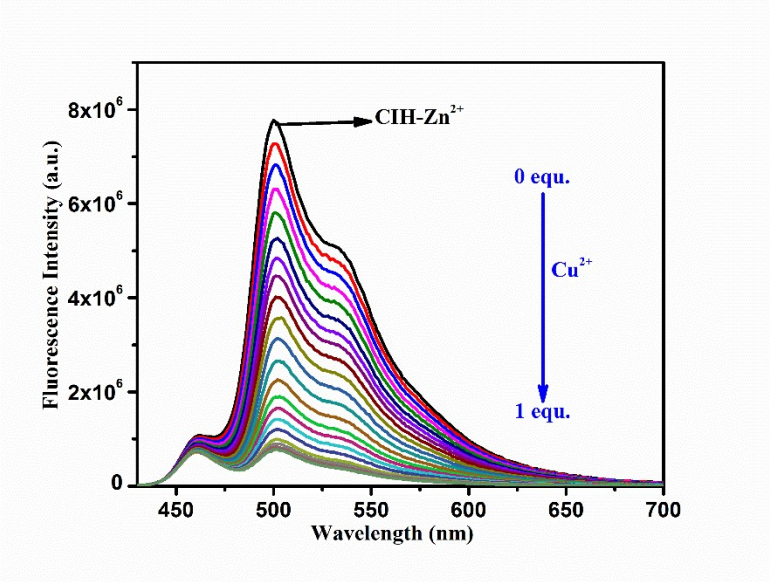


**Fig. S9** Fluorescence titration spectra of **CIH-$Zn^{2+}$** (20 μM) with $Cu^{2+}$ (0-1equiv.) in DMF:$H_2O$ (7:3, v/v, pH 7.4) HEPES buffer solution.

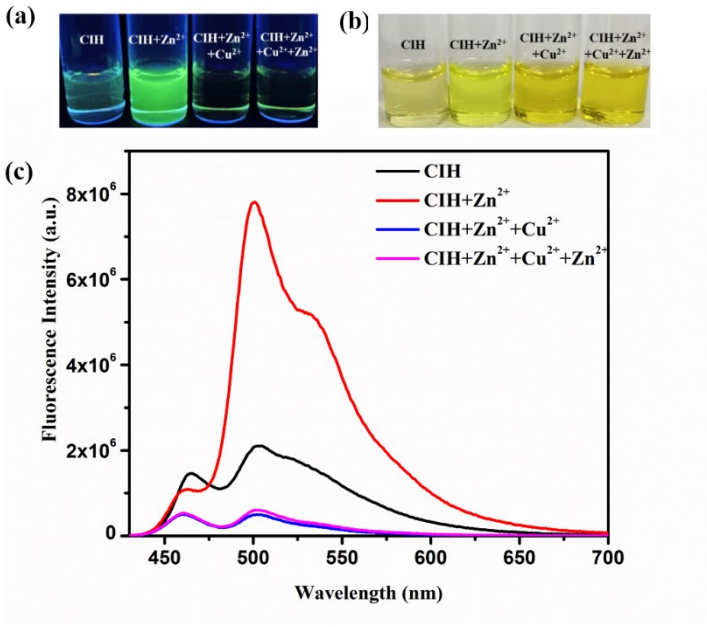


**Fig. S10** Images of **CIH, CIH-$Zn^{2+}$, CIH-$Zn^{2+}$-$Cu^{2+}$** and **CIH-$Zn^{2+}$-$Cu^{2+}$-$Zn^{2+}$** in DMF:$H_2O$ (7:3, v/v, pH 7.4) HEPES buffer solution under **(a)** UV- illumination and **(b)** Visible light. **(c)** Fluorescence spectra of **CIH** upon subsequent addition of $Zn^{2+}$ and $Cu^{2+}$.

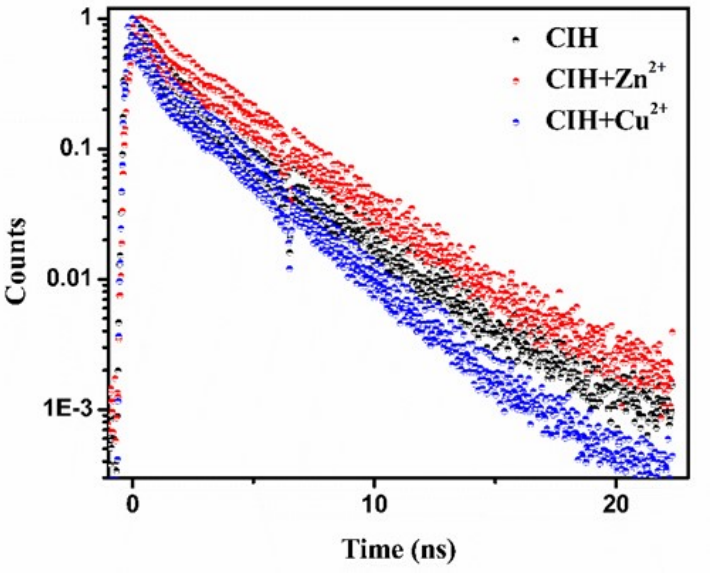


**Fig. S11** Time-resolved fluorescence decay profile of **CIH** in presence and absence of $Zn^{2+}$/$Cu^{2+}$, respectively in DMF:$H_2O$ (7:3, v/v, pH 7.4) HEPES buffer solution.

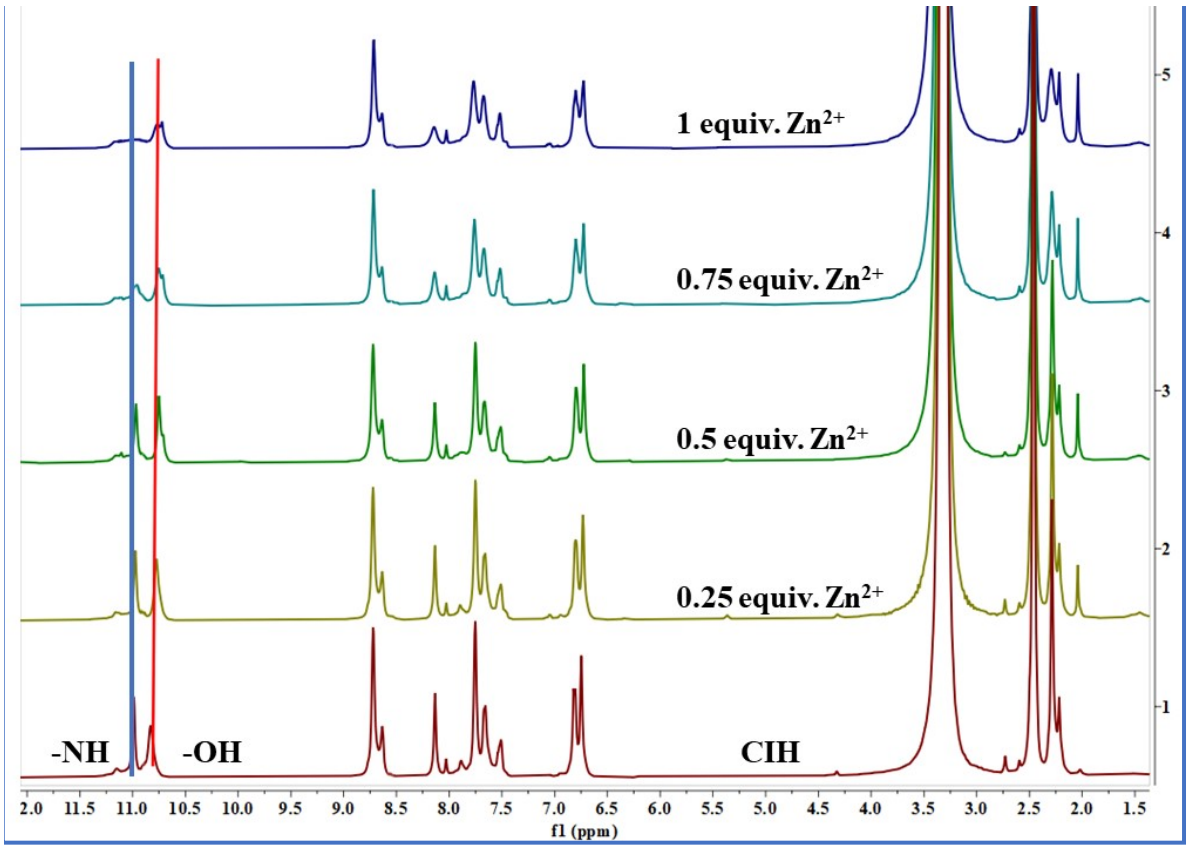


**Fig. S12** $^{1}$H NMR titration of **CIH** after addition of $Zn^{2+}$ (0-1 equiv.) in DMSO–$d_6$.

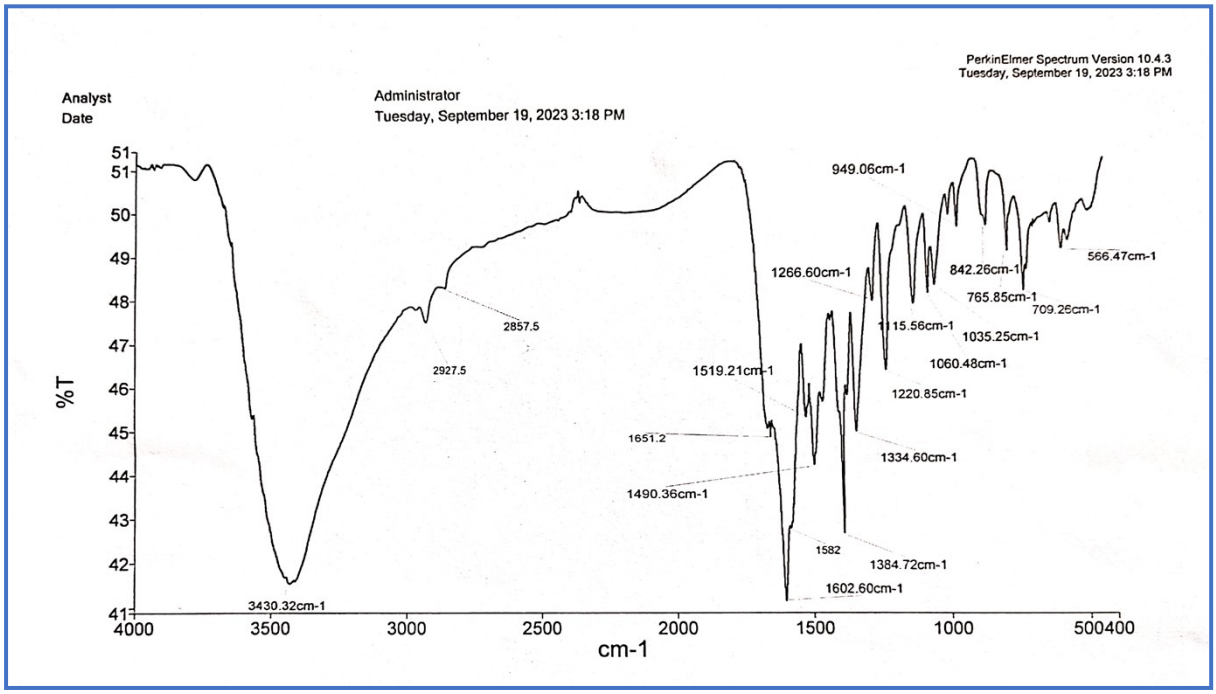


**Fig. S13** IR spectrum of **CIH**-$Zn^{2+}$ complex.

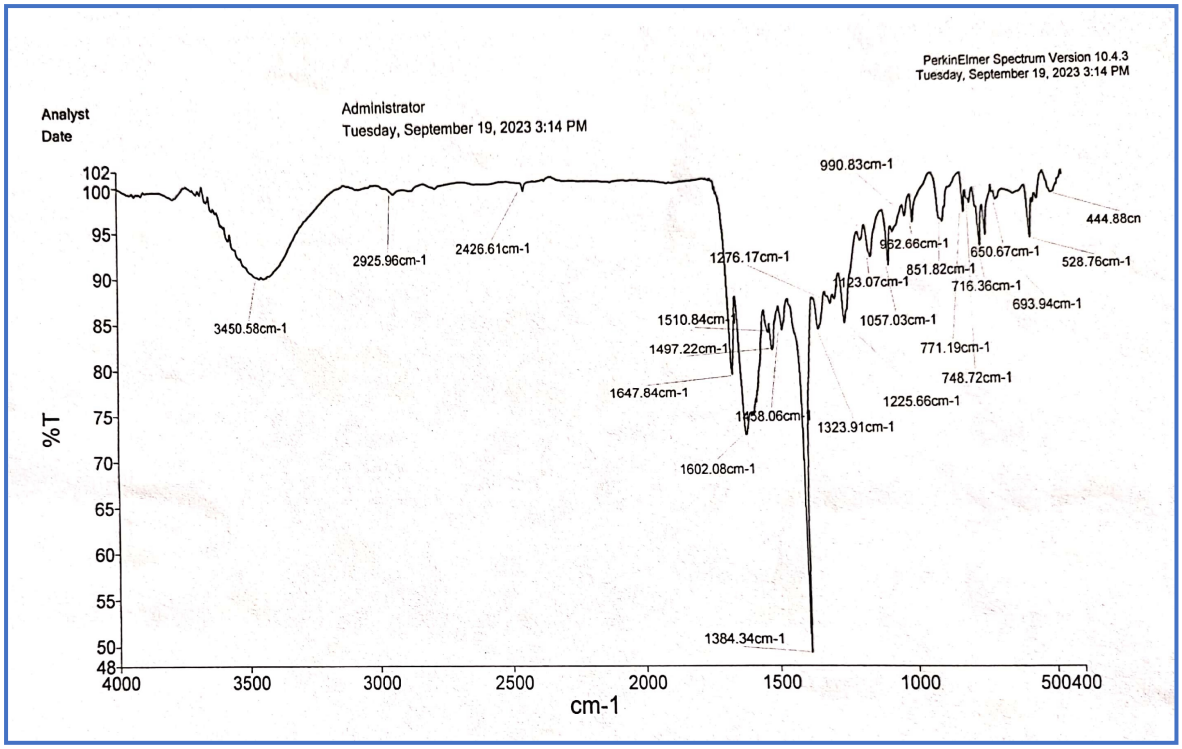


**Fig. S14** IR spectrum of **CIH**-$Cu^{2+}$ complex.

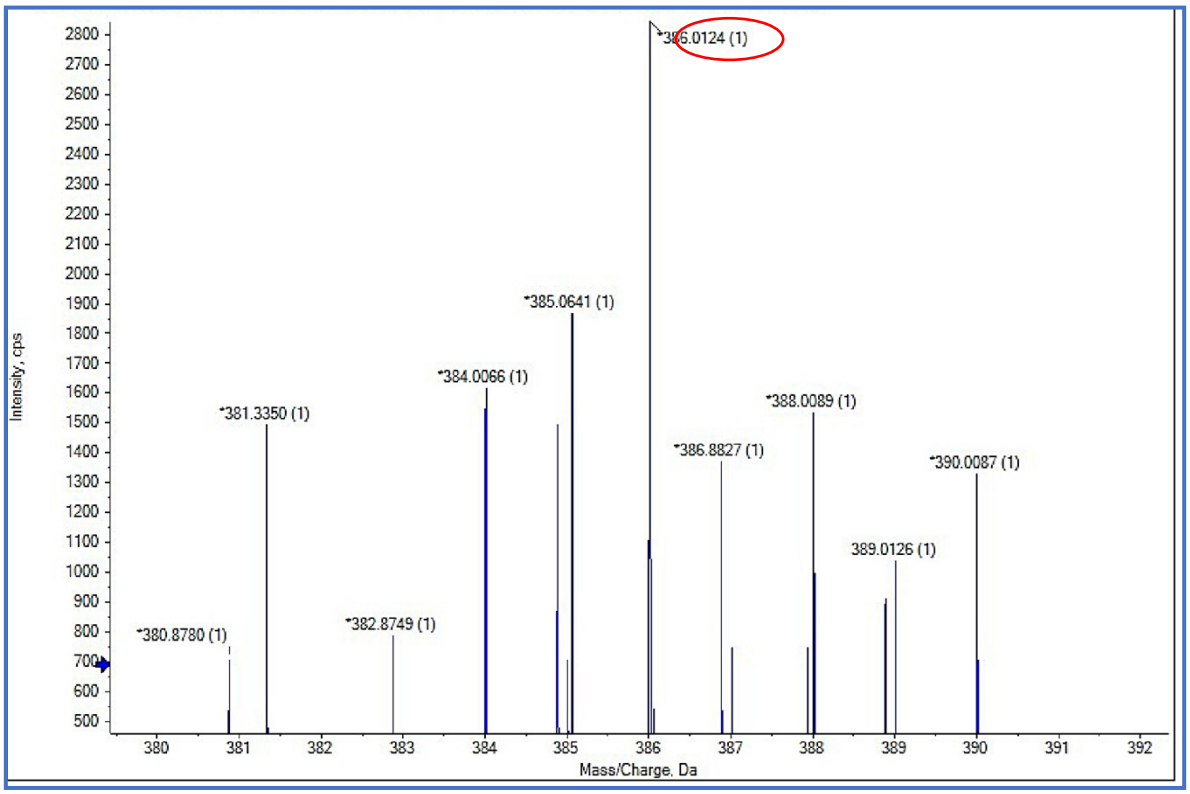


**Fig. S15** Mass spectrum of **CIH**-$Zn^{2+}$

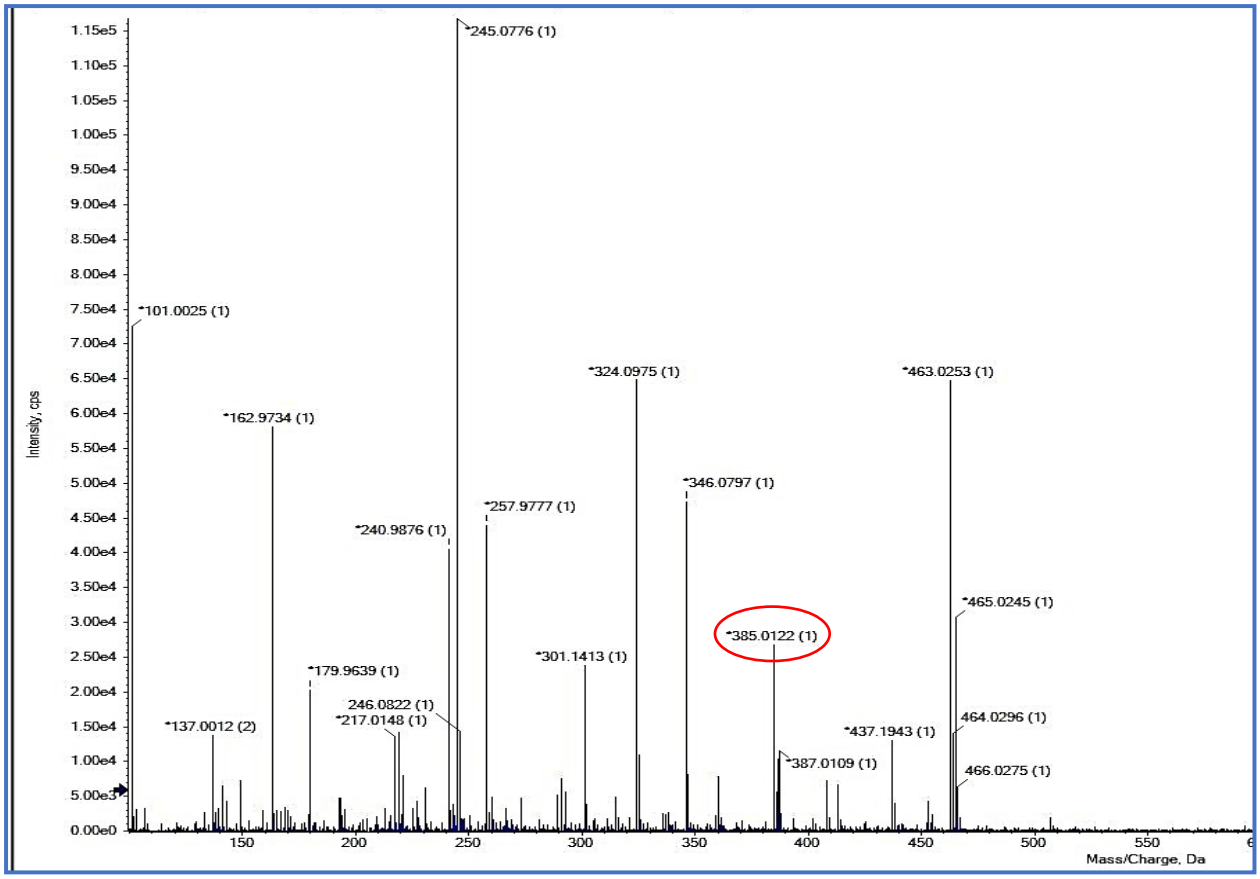


**Fig. S16** Mass spectrum of **CIH**-$Cu^{2+}$

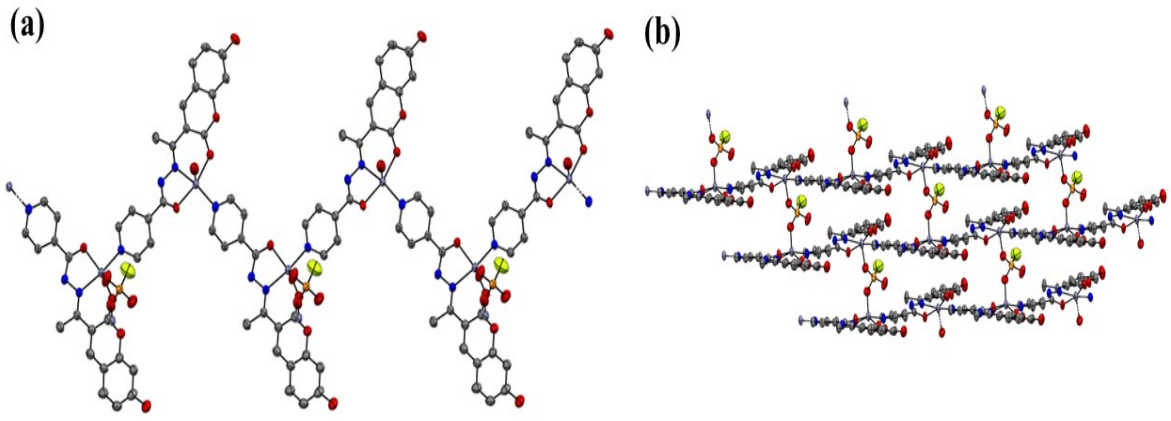


**Fig. S17 (a)** A one-dimensional supramolecular structure of **CIH**-$Zn^{2+}$ complex in a coordination polymer frame work **(b)** three-dimensional structure of **CIH**-$Zn^{2+}$ complex.

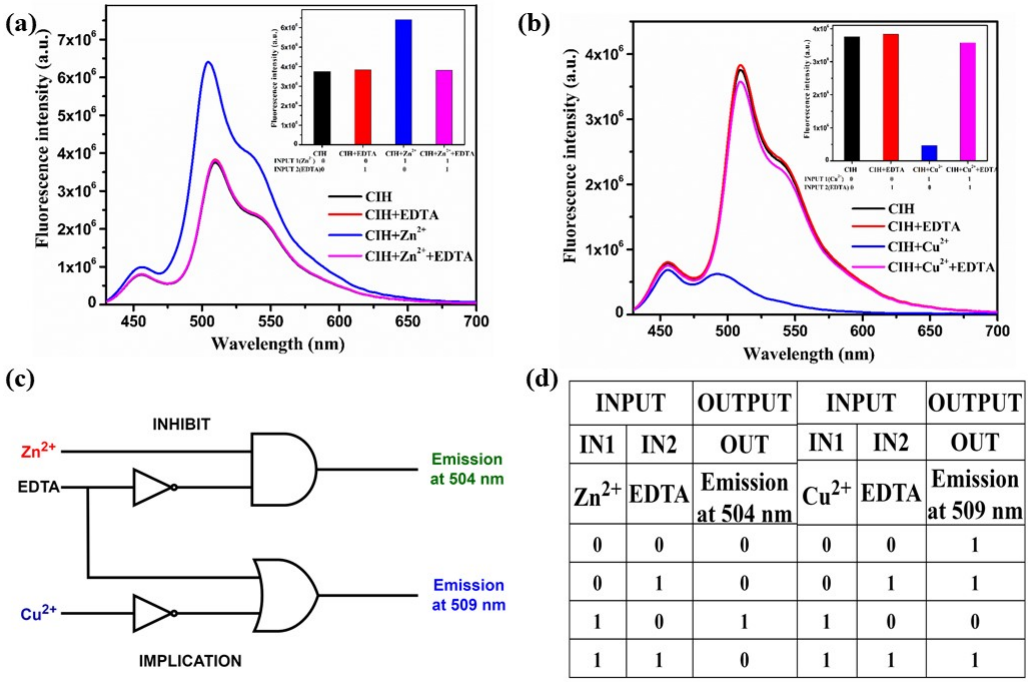


(d)

| INPUT | | OUTPUT | INPUT | | OUTPUT |
|---|---|---|---|---|---|
| IN1 | IN2 | OUT | IN1 | IN2 | OUT |
| $Zn^{2+}$ | EDTA | Emission at 504 nm | $Cu^{2+}$ | EDTA | Emission at 509 nm |
| 0 | 0 | 0 | 0 | 0 | 1 |
| 0 | 1 | 0 | 0 | 1 | 1 |
| 1 | 0 | 1 | 1 | 0 | 0 |
| 1 | 1 | 0 | 1 | 1 | 1 |

**Fig. S18 (a)** Changes in emission intensity of **CIH** (λex = 420 nm) in the presence and absence of $Zn^{2+}$ and EDTA. Inset: Diagram depicting the emission output at 504 nm. **(b)** Changes in the emission intensity of **CIH** (λex = 420 nm) in the presence and absence of $Cu^{2+}$ and EDTA. Inset: Diagram depicting the emission output at 509 nm. **(c)** Schematic illustration of INHIBIT and the IMPLICATION logic gate. **(d)** truth table.

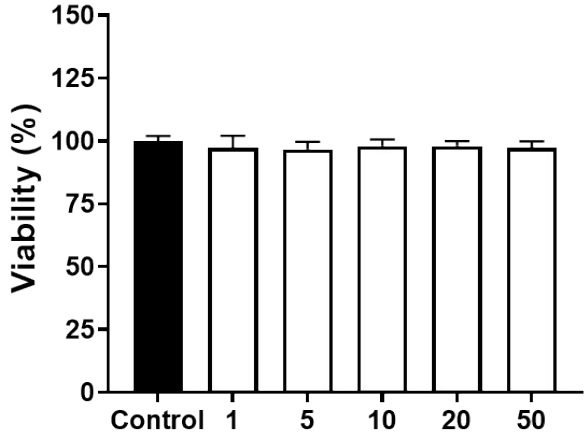


**Fig. S19** MTT assay plot showing treatment of SiHa cells with various concentration of **CIH** (1, 5, 10, 20 and 50 μM) for 4 h.

**Table S1** Quantum yields and fluorescence decay parameters of **CIH** before and after treatment with $Zn^{2+}$/$Cu^{2+}$ in DMF:$H_2O$ (7:3, v/v, pH 7.4) HEPES buffer solution.

| Sample | A | τ (ns) | < τ > (ns) | ϕ | Kr($^{-}$s) | Knr($^{-}$s) |
|---|---|---|---|---|---|---|
| **CIH** | 0.521 (A1)<br>0.348 (A2) | 1.075(τ1)<br>3.526 (τ2) | 2.055 | $10.41 \times 10^{-3}$ | $5.07 \times 10^{6}$ | $4.81 \times 10^{8}$ |
| **CIH**-$Zn^{2+}$ | 0.146 (A1)<br>0.637 (A2) | 0.99395(τ1)<br>3.41947(τ2) | 2.966 | $24.72 \times 10^{-3}$ | $8.33 \times 10^{6}$ | $3.29 \times 10^{8}$ |
| **CIH**-$Cu^{2+}$ | 0.482 (A1)<br>0.403 (A2) | 0.691 (τ1)<br>2.815 (τ2) | 1.658 | $2.70 \times 10^{-3}$ | $1.63 \times 10^{6}$ | $6.01 \times 10^{8}$ |

**Table S2**

Important crystallographic data of **CIH**-$Zn^{2+}$ complex

| | |
|---|---|
| CCDC No. | 2305336 |
| Empirical formula | $C_{34}H_{24}FN_6O_{11}PZn_2$ |
| Formula weight | 873.30 |
| Temperature (K) | 293 |
| Crystal system | triclinic |
| Space group | P-1 |
| a (Å) | 11.6235(3) |
| b (Å) | 12.0608(5) |
| c (Å) | 16.9201(7) |
| α (°) | 77.785(4) |
| β (°) | 87.986(3) |
| γ (°) | 77.824(3) |
| Volume (Å$^3$) | 2266.04(15) |
| Z | 2 |
| Density (g/cm$^3$) | 1.280 |
| μ (mm$^{-1}$) | 2.155 |

| | |
|---|---|
| F(000) | 884.0 |
| Crystal size ($mm^3$) | 0.025 × 0.02 × 0.01 |
| Radiation | Cu Kα (λ = 1.54184) |
| 2Θ range for data collection (°) | 5.344 to 144.238 |
| Reflections collected | 29742 |
| Independent reflections | 8843 [$R_{int}$ = 0.0494, $R_{sigma}$ = 0.0489] |
| Data/restraints/parameters | 8843/0/502 |
| Goodness-of-fit on $F^2$ | 1.054 |
| Final R indexes [I>=2σ (I)] | $R_1$ = 0.0665, $wR_2$ = 0.1947 |
| Final R indexes [all data] | $R_1$ = 0.0821, $wR_2$ = 0.2047 |

[a]$R_1 = \Sigma||Fo| - |Fc||\Sigma|Fo|$
[b]$R_2 = [\Sigma w(|F^2o| - |F^2c|)^2/\Sigma w|F^2o|^2]^{1/2}$

**Table S3** List of bond lengths for **CIH**-$Zn^{2+}$

| Atom | Atom | Length/Å | Atom | Atom | Length/Å |
|---|---|---|---|---|---|
| Zn1 | O4 | 1.989(3) | O8 | C32 | 1.323(6) |
| Zn1 | O3 | 2.055(3) | C13 | C12 | 1.493(6) |
| Zn1 | N4 | 2.053(4) | C13 | C14 | 1.395(6) |
| Zn1 | O9 | 1.965(4) | C13 | C15 | 1.386(7) |
| Zn1 | N1 | 2.092(4) | C26 | C27 | 1.454(6) |
| Zn2 | O6 | 2.144(3) | C26 | C28 | 1.373(6) |
| Zn2 | O5 | 2.068(3) | C26 | C24 | 1.454(6) |
| Zn2 | $O10^1$ | 2.075(4) | C23 | C22 | 1.501(6) |
| Zn2 | $N3^2$ | 2.071(4) | C28 | C29 | 1.413(7) |
| Zn2 | N6 | 2.088(4) | C24 | C25 | 1.507(6) |
| P1 | O10 | 1.450(4) | C17 | C15 | 1.387(6) |
| P1 | O9 | 1.448(4) | C22 | C21 | 1.391(6) |
| P1 | O11 | 1.454(4) | C22 | C20 | 1.394(7) |
| P1 | F1 | 1.473(5) | C29 | C34 | 1.385(7) |
| O7 | C27 | 1.355(5) | C29 | C30 | 1.408(7) |
| O7 | C34 | 1.377(6) | C34 | C33 | 1.389(7) |
| O6 | C27 | 1.235(5) | C5 | C3 | 1.379(7) |

| Atom | Atom | Length/Å | Atom | Atom | Length/Å |
|---|---|---|---|---|---|
| O5 | C23 | 1.265(5) | C5 | C6 | 1.386(7) |
| O2 | C5 | 1.379(6) | C21 | C19 | 1.383(6) |
| O2 | C9 | 1.357(6) | C8 | C10 | 1.486(7) |
| O4 | C12 | 1.274(5) | C8 | C9 | 1.449(7) |
| O3 | C9 | 1.216(6) | C8 | C7 | 1.363(7) |
| N5 | N6 | 1.391(5) | C10 | C11 | 1.499(7) |
| N5 | C23 | 1.306(6) | C14 | C16 | 1.380(7) |
| O1 | C1 | 1.343(6) | C1 | C3 | 1.385(7) |
| N3 | C17 | 1.327(6) | C1 | C2 | 1.405(8) |
| N3 | C16 | 1.349(6) | C30 | C31 | 1.354(7) |
| N6 | C24 | 1.299(6) | C7 | C6 | 1.415(7) |
| N2 | N1 | 1.395(5) | C31 | C32 | 1.394(8) |
| N2 | C12 | 1.312(6) | C6 | C4 | 1.405(7) |
| N4 | C19 | 1.333(6) | C20 | C18 | 1.352(7) |
| N4 | C18 | 1.349(6) | C32 | C33 | 1.410(7) |
| N1 | C10 | 1.301(6) | C2 | C4 | 1.359(8) |

**Table S4** List of bond angles for **CIH**-$Zn^{2+}$

| Atom | Atom | Atom | Angle/° | Atom | Atom | Atom | Angle/° |
|---|---|---|---|---|---|---|---|
| O4 | Zn1 | O3 | 148.18(17) | C28 | C26 | C24 | 119.8(4) |
| O4 | Zn1 | N4 | 96.27(15) | O5 | C23 | N5 | 128.0(4) |
| O4 | Zn1 | N1 | 78.41(14) | O5 | C23 | C22 | 117.7(4) |
| O3 | Zn1 | N1 | 83.86(15) | N5 | C23 | C22 | 114.3(4) |
| N4 | Zn1 | O3 | 90.24(15) | O7 | C27 | C26 | 119.1(4) |
| N4 | Zn1 | N1 | 157.78(18) | O6 | C27 | O7 | 113.3(4) |
| O9 | Zn1 | O4 | 99.50(17) | O6 | C27 | C26 | 127.6(4) |
| O9 | Zn1 | O3 | 109.76(18) | C26 | C28 | C29 | 123.9(4) |
| O9 | Zn1 | N4 | 101.15(19) | N6 | C24 | C26 | 120.3(4) |
| O9 | Zn1 | N1 | 101.01(19) | N6 | C24 | C25 | 121.9(4) |
| O5 | Zn2 | O6 | 161.42(12) | C26 | C24 | C25 | 117.9(4) |
| O5 | Zn2 | $O10^{1}$ | 94.16(16) | N3 | C17 | C15 | 122.2(4) |
| O5 | Zn2 | $N3^{2}$ | 95.87(14) | C21 | C22 | C23 | 120.9(4) |
| O5 | Zn2 | N6 | 77.52(13) | C21 | C22 | C20 | 117.6(4) |

| Atom | Atom | Atom | Angle/° | Atom | Atom | Atom | Angle/° |
|---|---|---|---|---|---|---|---|
| O10[1] | Zn2 | O6 | 91.56(15) | C20 | C22 | C23 | 121.5(4) |
| O10[1] | Zn2 | N6 | 98.27(15) | C34 | C29 | C28 | 116.9(4) |
| N3[2] | Zn2 | O6 | 101.45(14) | C34 | C29 | C30 | 118.1(4) |
| N3[2] | Zn2 | O10[1] | 93.24(17) | C30 | C29 | C28 | 124.8(4) |
| N3[2] | Zn2 | N6 | 167.08(16) | O7 | C34 | C29 | 120.7(4) |
| N6 | Zn2 | O6 | 84.17(13) | O7 | C34 | C33 | 117.1(4) |
| O10 | P1 | O11 | 112.1(2) | C29 | C34 | C33 | 122.2(5) |
| O10 | P1 | F1 | 109.4(3) | O2 | C5 | C3 | 116.9(5) |
| O9 | P1 | O10 | 107.5(3) | O2 | C5 | C6 | 119.0(4) |
| O9 | P1 | O11 | 110.0(3) | C3 | C5 | C6 | 124.1(5) |
| O9 | P1 | F1 | 107.9(3) | C19 | C21 | C22 | 119.2(4) |
| O11 | P1 | F1 | 109.9(3) | C9 | C8 | C10 | 121.3(4) |
| C27 | O7 | C34 | 122.7(4) | C7 | C8 | C10 | 121.1(5) |
| C27 | O6 | Zn2 | 124.5(3) | C7 | C8 | C9 | 117.7(5) |
| C23 | O5 | Zn2 | 109.1(3) | N1 | C10 | C8 | 119.7(4) |
| C9 | O2 | C5 | 123.4(4) | N1 | C10 | C11 | 122.3(4) |
| C12 | O4 | Zn1 | 111.0(3) | C8 | C10 | C11 | 117.9(4) |
| C9 | O3 | Zn1 | 126.8(3) | O2 | C9 | C8 | 118.7(4) |
| P1 | O10 | Zn2[3] | 143.0(3) | O3 | C9 | O2 | 112.4(4) |
| C23 | N5 | N6 | 111.0(4) | O3 | C9 | C8 | 128.9(5) |
| C17 | N3 | Zn2[4] | 121.9(3) | C16 | C14 | C13 | 119.8(4) |
| C17 | N3 | C16 | 118.8(4) | N3 | C16 | C14 | 122.0(4) |
| C16 | N3 | Zn2[4] | 119.3(3) | O1 | C1 | C3 | 116.9(5) |
| N5 | N6 | Zn2 | 112.0(3) | O1 | C1 | C2 | 122.4(5) |
| C24 | N6 | Zn2 | 132.6(3) | C3 | C1 | C2 | 120.7(5) |
| C24 | N6 | N5 | 115.4(4) | C13 | C15 | C17 | 120.0(4) |
| C12 | N2 | N1 | 109.7(4) | C31 | C30 | C29 | 121.0(5) |
| C19 | N4 | Zn1 | 118.2(3) | N4 | C19 | C21 | 122.3(4) |
| C19 | N4 | C18 | 118.2(4) | C8 | C7 | C6 | 122.5(5) |
| C18 | N4 | Zn1 | 122.6(3) | C30 | C31 | C32 | 120.7(5) |
| P1 | O9 | Zn1 | 140.6(3) | C5 | C3 | C1 | 117.3(5) |
| N2 | N1 | Zn1 | 111.6(3) | C5 | C6 | C7 | 118.7(5) |
| C10 | N1 | Zn1 | 130.1(3) | C5 | C6 | C4 | 116.5(5) |

| Atom | Atom | Atom | Angle/° | Atom | Atom | Atom | Angle/° |
|---|---|---|---|---|---|---|---|
| C10 | N1 | N2 | 116.7(4) | C4 | C6 | C7 | 124.8(5) |
| C14 | C13 | C12 | 123.1(4) | C18 | C20 | C22 | 119.8(5) |
| C15 | C13 | C12 | 119.6(4) | O8 | C32 | C31 | 120.8(5) |
| C15 | C13 | C14 | 117.3(4) | O8 | C32 | C33 | 119.2(5) |
| O4 | C12 | N2 | 127.7(4) | C31 | C32 | C33 | 120.0(5) |
| O4 | C12 | C13 | 116.4(4) | C34 | C33 | C32 | 118.0(5) |
| N2 | C12 | C13 | 115.9(4) | C4 | C2 | C1 | 119.8(5) |
| C27 | C26 | C24 | 123.4(4) | N4 | C18 | C20 | 122.8(5) |
| C28 | C26 | C27 | 116.7(4) | C2 | C4 | C6 | 121.6(6) |

**Table S5** Comparison of **CIH** with the previously reported sensors.

| S. No. | Working media | Analyte | Detection limit (M) | Applications | Reversibility | Ref. |
|---|---|---|---|---|---|---|
| 1 | $CH_3OH$: $H_2O$ (9:1, pH 7.4) | $Zn^{2+}$, $Cu^{2+}$ | $Zn^{2+}$: $3.21 \times 10^{-8}$ $Cu^{2+}$: $2.13 \times 10^{-8}$ | Logic gates, live cell imaging | Yes | 5 |
| 2 | $CH_3CN$ | $Zn^{2+}$, $Cu^{2+}$ | $Zn^{2+}$: $2.41 \times 10^{-6}$ $Cu^{2+}$: $4.23 \times 10^{-6}$ | Logic gates | Yes | 6 |
| 3 | THF:$H_2O$ (5:95) | $Zn^{2+}$, $Cu^{2+}$ | $Zn^{2+}$: $1.8 \times 10^{-6}$ $Cu^{2+}$: $2.3 \times 10^{-7}$ | live cell imaging | No | 7 |
| 4 | DMSO:water (1:1) | $Zn^{2+}$, $Cu^{2+}$ | $Zn^{2+}$: $3.5 \times 10^{-8}$ $Cu^{2+}$: $1.46 \times 10^{-6}$ | Logic gates, live cell imaging | Yes | 8 |
| 5 | DMSO/$H_2O$ (4:1, v/v) | $Zn^{2+}$, $Cu^{2+}$ | $Zn^{2+}$: $6.8 \times 10^{-8}$ $Cu^{2+}$: $2.3 \times 10^{-8}$ | Logic gates | No | 9 |
| 6 | HEPES Buffer | $Zn^{2+}$, $Cu^{2+}$ | $Zn^{2+}$: $2.29 \times 10^{-9}$ $Cu^{2+}$: $3.67 \times 10^{-9}$ | Logic gates, live cell imaging | Yes | 10 |
| 7 | HEPES Buffer | $Zn^{2+}$, $Cu^{2+}$ | $Zn^{2+}$: $13.2 \times 10^{-9}$ $Cu^{2+}$: $4.1 \times 10^{-9}$ | Logic gates, live cell imaging | No | 11 |
| 8 | EtOH: $H_2O$ (1:99) | $Zn^{2+}$, $Cu^{2+}$ | $Zn^{2+}$: $72 \times 10^{-9}$ $Cu^{2+}$: $141 \times 10^{-9}$ | Logic gates, live cell imaging | Yes | 12 |
| 9 | DMF:$H_2O$ (7:3, pH 7.4) HEPES | $Zn^{2+}$, $Cu^{2+}$ | $Zn^{2+}$: $3.49 \times 10^{-9}$ $Cu^{2+}$: $5.36 \times 10^{-9}$ | Logic gates, live cell imaging, mitotracking | Yes | This Work |

## References


1 G. L. Long and J. D. Winefordner, *Anal. Chem.*, 2008, **55**, 712A-724A.

2 H. A. Benesi and J. H. Hildebrand, *J. Am. Chem. Soc.*, 2002, **71**, 2703–2707.

3 K. Nawara and J. Waluk, *Anal. Chem.*, 2017, **89**, 8650–8655.

4 K. R. Barqawi, Z. Murtaza and T. J. Meyer, *Calculation of Relative Nonradiative Decay Rate Constants from Emission Spectral Profiles. Polypyridyl Complexes of Ru( I I )*, 1991, vol. 95.

5 P. Das, S. Singh Rajput, M. Das, S. Laha, I. Choudhuri, N. Bhattacharyya, A. Das, B. Chandra Samanta, M. Mehboob Alam and T. Maity, *J. Photochem. Photobiol. A Chem.*, 2022, **427**, 113817.

6 R. Arabahmadi, *J. Photochem. Photobiol. A Chem.*, 2022, **426**, 113762.

7 B. Zha, S. Fang, H. Chen, H. Guo and F. Yang, *Spectrochim. Acta, Part A,* 2022, **269**, 120765.

8 J. Shree Ganesan, S. Gandhi, K. Radhakrishnan, A. Balasubramaniem, M. Sepperumal and S. Ayyanar, *Spectrochim. Acta, Part A,* 2019, **219**, 33-43

9 Y. Sun, W. Ding, J. Li, Y. Jia, G. Guo and Z. Deng, *J. Mol. Struct.*, 2022, **1252**, 132219.

10 P. Ghorai, S. Banerjee, D. Nag, S. K. Mukhopadhyay and A. Saha, *J. Lumin.*, 2019, **205**, 197–209.

11 P. Wang, S. Xue and X. Yang, *Microchemical Journal*, 2020, **158**, 105147.

12 X. He, Q. Xie, J. Fan, C. Xu, W. Xu, Y. Li, F. Ding, H. Deng, H. Chen and J. Shen, *Dyes and Pigments*, 2020, **177**, 108255.